# Temperature-Dependent Growth of Gelatin–Poly(galacturonic acid) Multilayer Films and Their Responsiveness to Temperature, pH, and NaCl

**ARTICLE** *in* MACROMOLECULES · NOVEMBER 2010

Impact Factor: 5.8 · DOI: 10.1021/ma101466w



**3 AUTHORS:**

Marta Westwood
Union Chimique Belge (UCB)
**6** PUBLICATIONS **45** CITATIONS
SEE PROFILE

A. Patrick Gunning
Institute of Food Research
**115** PUBLICATIONS **3,042** CITATIONS
SEE PROFILE

Roger Parker
Institute of Food Research
**91** PUBLICATIONS **2,727** CITATIONS
SEE PROFILE

10582 *Macromolecules* **2010**, *43*, 10582–10593
DOI: 10.1021/ma101466w

Macromolecules
ARTICLE

# Temperature-Dependent Growth of Gelatin−Poly(galacturonic acid) Multilayer Films and Their Responsiveness to Temperature, pH, and NaCl

**Marta Westwood,* A. Patrick Gunning, and Roger Parker**

*Institute of Food Research, Norwich Research Park, Colney, Norwich NR4 7UA, United Kingdom*

*Received July 1, 2010; Revised Manuscript Received October 12, 2010*

ABSTRACT: Temperature-dependent formation of gelatin−poly(galacturonic acid) (PGA) multilayer films based on the layer-by-layer approach and their stability to changes in temperature, pH, and NaCl concentration were investigated for the first time using quartz crystal microbalance with dissipation monitoring (QCMD). Changes in the viscoelastic properties of the gelatin−PGA films with temperature were also observed using atomic force microscopy (AFM). Four different assembly temperatures ranging from 20 to 37 °C were chosen, and the findings revealed that the assembly temperature was crucial to gelatin−PGA multilayer film formation. The highest amount adsorbed and consequently the thickest gelatin−PGA assemblies were formed at 20 °C, whereas limited growth was observed for gelatin−PGA films assembled at 37 °C. Although the experimental conditions favored electrostatic interactions to be the driving force during the gelatin−PGA assembly, the inhibited multilayer growth observed for layers formed at the temperature of 30 and 37 °C clearly indicated very weak electrostatic interactions between gelatin and PGA and the continuous multilayer growth at lower temperatures was mainly due to hydrogen bonding. The stability of assembled gelatin−PGA multilayer films to various environmental stresses was found to be significantly influenced by the changes in temperature. At low temperatures the behavior of gelatin was dominated by helix formation and association through hydrogen bonding. Raising the temperature promoted melting of the helix, disruption of the multilayer network, and disassembly of the films, which was also indicated by AFM study. In terms of the responsiveness to pH and salt, this study showed that gelatin−PGA multilayer films fabricated at 20 °C underwent almost completely reversible alternate (de)swelling changes. In contrast, gelatin−PGA multilayer films formed at 25 °C showed a partial decomposition when exposed to various pH and salt concentrations.

## Introduction

Gelatin is a natural polymer and a product of collagen denaturation. It is relatively cheap and has been used widely in the food, tissue engineering, photographic, biochemical and pharmaceutical industries as a binder, stabilizer, and gelling agent. Because of the many useful functional properties of gelatin, such as biodegradability, hydrophilicity, nontoxicity, and biocompatibility, it has many potential applications as a major component in controlled delivery systems.[1−6] Gelatin is a weak polyampholyte with a nonuniform distribution of amino acids. Like all proteins gelatin has an isoelectric point (IEP), above which it has a net positive charge and below which it has a net negative charge. There are two types of gelatin that are produced commercially, and the type is determined by the collagen pretreatment method. Gelatin of type A is obtained through acid hydrolysis and is characterized by an IEP occurring at pH 6−9. In contrast, type B gelatin is prepared by alkali hydrolysis and has an IEP at pH 5.[6]

In aqueous solution at room temperature the structure of gelatin is determined by two types of intermolecular interactions: electrostatic and nonelectrostatic. Electrostatic interactions result from the presence of charges and charge distributions on the polypeptide chain. On cooling hot solutions, hydrogen bonds formed between the amino acid units on adjacent chains cause the gelatin chains to adopt a triple-helical structure and, at sufficiently high concentrations, to associate to form physical gels.[7−10]

Considerable literature related to the adsorption process of gelatin onto well-defined substrates has shown that the structure of an adsorbed layer of gelatin is strongly dependent on the pH, temperature, ionic strength, and concentration of the solution.[7−10] A study conducted by Curme and Natale, detailing the influence of the ionizing groups on the adsorption of gelatin onto silver bromide sols, indicated that gelatin adsorption showed a maximum in the vicinity of the IEP.[11] Kamiyama and Israelachvili[12] reported that gelatin adsorption onto mica is driven primarily by electrostatic interactions, and Su et al.[13] demonstrated that gelatin can adsorb to either positively or negatively charged substrates depending on the pH of the gelatin solution. Lately, Noel et al.[14] reported the sequential deposition of pectin and protein, including gelatin using the layer-by-layer approach, and de Villiers et al.[1] included gelatin as a component of the polylelectrolyte multilayer assembly used to encapsulate dexamethasone.

Layer-by-layer assembly has been used extensively to construct multilayer thin films from various molecules, including, among others, weak polyelectrolytes and (poly)ampholytes.[15−24] Most commonly the process involves the use of at least two oppositely charged species assembled in an alternating fashion driven mainly by electrostatic interaction. Extensive studies have revealed that the formation of multilayer films based on weak polyelectrolytes enables a greater control over the film thickness, morphology, surface, internal composition, and stability by manipulation of the assembly conditions.[17,25−28] Rubner et al.[29] and Moffat et al.[30] have shown pH-induced changes in the stability and morphology of multilayer films formed on a flat substrate. Dubas and Schlenoff[24] reported swelling behavior, leading to the disassembly of a polyelectrolyte network consisting of one strong and one weak polyelectrolyte, at a salt concentration greater than 0.6 M

*Corresponding author: Tel +44 1603 255000, Fax +44 1603 507723, e-mail marta.westwood@bbsrc.ac.uk.

 Published on Web 11/23/2010 

NaCl. Möhwald et al.[31] reported that the permeation of chemicals through the shells of multilayer capsules can be tuned by changes in pH.

Although the layer-by-layer approach commonly refers to multilayer films assembled through electrostatic interactions, hydrogen-bonding interactions are recognized as an alternative route to fabricate multilayer films.[32−38] The earliest published studies by Rubner et al.[37] on hydrogen-bonded assemblies showed that multilayer films fabricated via hydrogen bonding form lower density films when compared to similar films formed via electrostatic interactions. Sukhishvili et al.[38] investigated hydrogen-bonded multilayer growth for a number of polyelectrolyte multilayer films and showed that the films could be disassembled in a controlled manner at higher pH values. Schlenoff et al.[24] have reported incomplete dissociation of electrostatically assembled multilayer films in response to pH challenge that was due to formation of hydrogen bonding between polyelectrolytes at low pH values. Caruso et al.[39] fabricated hybrid structures that were composed of electrostatically and hydrogen-bonded assembled layers and demonstrated pH-induced decomposition of hydrogen-bonded polymer layers sandwiched between electrostatically bound layers.

The increasing interest in recent years for controlled delivery systems in food-related applications has provided a drive to develop novel delivery systems fabricated with the layer-by-layer technique. This would enable the encapsulation of nutrients, flavors, and other bioactives, which can be released by triggers such as temperature, or the variation in pH and ionic strength along the gastrointestinal tract. However, food-related controlled delivery systems require the use of natural-based films, and with this aim in mind, the present studies have been made on multilayer films consisting of the weak polyampholyte gelatin and weak polyanion poly(galacturonic acid) (PGA). PGA is a form of pectin which is essentially a linear polysaccharide extracted from the cell walls of edible plants. The extracts predominantly contain linear chains of D-galacturonic acid units with small quantities of neutral sugars. In pectin, the PGA is partially esterified with methyl groups, and the free carboxylate groups enable pectin to form electrostatic interactions with polycations.

In terms of controlled delivery it is necessary to understand how assembly parameters, such as temperature, pH, and ionic strength, affect the multilayer assembly and also what changes occur to the multilayer structures in response to environmental stresses. Because of the ability of gelatin to form both electrostatic and hydrogen-bonded interactions, it is very likely that this will have a significant effect on the formation and stability of gelatin-based multilayer films. Thus, we have investigated the effect of temperature on the growth of gelatin−PGA multilayers. We then investigated the stability of these films in response to changes in temperature, pH, and ionic strength, using the QCMD and AFM that provided information on changes in the hydrated mass and the viscoelastic properties of deposited films.

## Materials and Methods

**Solution Preparation.** Poly(galacturonic acid) (PGA) with a molecular weight 25−50 kDa was supplied by Fluka Biochemika. Porcine gelatin type A with average molecular weight of 110 kDa and IEP of 8.8 was obtained from Rousselot NV, Gent. Poly(L-lysine hydrobromide) (PLL) with a mean degree of polymerization 70, sodium phosphate (monobasic anhydrous), sodium chloride, and acetic acid were obtained from Sigma, hydrochloric acid was obtained from Merck, and potassium chloride and sodium acetate were obtained from BDH. The reagents were analytical grade and were used without further purification. The aqueous solutions used for the multilayer assembly were prepared by dissolving the biopolymers at a concentration of 0.6 mg $mL^{-1}$ in10 mM pH 7.0 sodium phosphate solution containing 30 mM NaCl. Gelatin solutions were prepared by heating gelatin dispersions to ~50 °C until the gelatin was fully dissolved and then cooling the solution to room temperature. The pH of the PGA and gelatin solutions were 7.0 and 5.0, respectively, adjusting the pH using 0.1 M NaOH where necessary. For the pH responsiveness studies, HCl/KCl and acetic acid/sodium buffers were prepared at the required pH, each containing 30 mM NaCl. For the NaCl responsiveness studies, 10 mM, pH 7.0 sodium phosphate solutions with NaCl concentrations ranging from 30 to 500 mM were prepared.

**Multilayer Formation.** The multilayer structures were fabricated on a silicon dioxide substrate using layer-by-layer assembly[15] at four different temperatures ranging from 20 to 37 °C. Prior to deposition the substrate surfaces were cleaned using a UV-ozone chamber (Bioforce Nanosciences, Inc., Ames, IA), then rinsed thoroughly with water, and dried with $N_2$. For all of the multilayer films the base layer was formed by deposition of PLL. In order to enhance the electrostatic interactions between PGA and gelatin, PGA was dissolved at pH 7.0, and gelatin was dissolved at pH 5.0. At pH 7.0 PGA is fully charged. Although gelatin with an IEP at 8.1 will carry a net positive charge at pH 7.0, pH 5.0 was chosen to increase the net positive charge. The multilayer assembly of gelatin−PGA was produced by alternating exposure of the PLL-coated substrate to a PGA and then to a gelatin solution. Each biopolymer deposition step was followed by a two-stage sodium phosphate rinse. Following a PGA deposition, the surface was first rinsed with a pH 7.0 sodium phosphate solution and then with a pH 5.0 sodium phosphate solution. Following a gelatin deposition, the surface was first rinsed with a pH 5.0 sodium phosphate solution and then with a pH 7.0 sodium phosphate solution. Each exposure lasted 4 min. A total of 10 layers were deposited, which corresponds to 5 bilayers (one bilayer is formed by deposition of polycation and polyanion layers) following the approach of Burke and Barrett.[40] To summarize, in our study the films investigated consisted of PLL−PGA−(gelatin−PGA)$_4$, with PGA as the top layer.

**Multilayer Responsiveness Studies.** The effect of temperature on the gelatin−PGA multilayers was studied by exposing the films to changes in temperature—starting from the temperature at which the multilayer was fabricated, increasing the temperature in 4 °C increments up to 37 °C, and then returning to the multilayer fabrication temperature in 4 °C decrements. To assess the multilayer response to pH, the assemblies were first exposed to solutions of decreasing pH, starting from 7.0 down to 1.6. In order to study the reversibility of the process, the pH was then increased in the same steps back to 7.0. To assess the multilayer response to NaCl, the gelatin−PGA multilayer assemblies were exposed to solutions of increasing salt concentration ranging from 30 to 500 mM NaCl. Each exposure lasted 5 min. To examine the reversibility of the process, the salt concentration was decreased in the same steps back to 30 mM NaCl.

The change of hydrated mass observed in response to the exposure to environmental stress (temperature, pH, or salt concentration) was defined as

$$s = \frac{m}{m_0} \tag{1}$$

where $m_0$ and $m$ represent the hydrated mass obtained before and after the response to temperature, pH, or salt, respectively.

After the response studies the surfaces were cleaned with 2% v/v Hellmanex, rinsed with water, exposed to an UV-ozone treatment, rinsed again with water, and finally dried with $N_2$

**Quartz Crystal Microbalance with Dissipation Monitoring (QCMD).** The multilayer assembly processes were monitored using a D300 QCMD (Q-Sense AB, Västra Frölunda, Sweden) with a QAFC 302 axial flow measurement chamber as described elsewhere.[25] Silicon dioxide coated AT-cut quartz crystals sandwiched between gold electrodes as supplied by (QSX-303,

Q-Sense AB, Västra Frölunda, Sweden) were used as the substrate. This QCMD sensor was placed in the measurement chamber, and an ac voltage was applied to excite the fundamental resonant frequency (~5 MHz) of the crystal and its overtones (3, 5, and 7). Each layer was formed during a 4 min exposure of the sensor surface to a biopolymer solution, and each deposition step was followed by a two-stage rinse, as described above. The assembly and environmental response studies were carried out in real time by monitoring changes in the oscillation frequency of the crystal. A decrease in oscillation frequency indicates the adsorption of mass onto the QCMD sensor. If the mass is deposited evenly and forms a rigid elastic layer, then the negative frequency changes are proportional to the hydrated mass deposited ($\Delta m$) as described by the Sauerbrey equation.[41]

$$\Delta m = \frac{-C\Delta f_n}{n} \quad (2)$$

where $C$ is the mass sensitivity constant ($C = 17.7\ \mathrm{ng\,cm^{-2}\,Hz^{-1}}$ for a 5 MHz crystal[42] and $\Delta f_n$ the frequency shift of the $n^{\mathrm{th}}$ overtone). For viscoelastic materials, the Sauerbrey relation leads to an underestimation of the deposited hydrated mass, and under these conditions, a more detailed analysis was performed using the Voigt model with the QTools modeling package (Q-Sense AB, Västra Frölunda, Sweden).

**AFM and Force Spectroscopy.** Studies were made using a combined AFM−inverted optical microscope (MFP-3D BIO Asylum Research Inc.). The instrument was fitted with a heating stage which maintained the sample temperature to within 0.1 °C of the set point. For mechanical mapping of the sample surface data were captured in a "force−volume" imaging mode (at a rate of 10 $\mu\mathrm{m\,s^{-1}}$ in the $z$ direction and a scan rate of 1 Hz) using a cantilever with a 30 $\mu$m colloidal glass bead attached adjacent to the tip. The colloidal glass sphere was attached to the cantilever with epoxy resin using a method described previously.[43] In this mode a force versus distance curve is performed at each imaging point (i.e., the instrument ramps the $Z$ piezo element of the scanner by a predetermined amount at each imaging point over a selected scan area and records the subsequent deflection of the cantilever as it is pushed into and then retracted away from the sample surface). The force−distance data were captured in "relative" mode which ensures that at each point in the image the sample surface is subjected to the same loading force on approach before the retraction part of the cycle is commenced. "Force−volume" imaging produces a matrix of curves of force (cantilever deflection) versus distance which relate to the image coordinates. This allows features in the force−distance data to be matched to sample topography. The "stiffness" images presented here are 40 × 40 pixels laterally, and the associated matrix of cantilever deflection−distance curves contain around 3000 points. Raw data of cantilever deflection−piezo displacement captured by the AFM were converted into force−distance using experimentally determined values for INVOLS[44] and spring constant, $k$.[45,46] Relative "stiffness" data were generated by fitting the deflection region (i.e., where the cantilever was bending in response to the sample surface) of the force curves between 10% and 90% of the range traveled. The fit produces a single "stiffness" value for each curve which is then plotted as an intensity at the $x$, $y$ coordinate over which it was recorded in the "stiffness" maps. At the ionic strength used for these experiments long-range electrostatic forces will be effectively screened to very short distances, meaning that the data measured from the force curves comes principally from sample deformation.

## Results and Discussion

**Temperature-Dependent Multilayer Assembly.** The temperature-dependent layer-by-layer assembly of all gelatin−PGA multilayer films were monitored in real time using QCMD. The films under investigation were formed at different temperatures: 20, 25, 30, and 37 °C. The simultaneous measurements of the quartz crystal oscillator frequency shifts ($\Delta f_n/n$) and dissipation ($\Delta D_n$) recorded at the three overtones ($n$ = 3, 5, 7) during the assembly are shown in Figure 1.

During the formation of gelatin−PGA multilayer films at 20 °C, a continuous decrease in $\Delta f_n/n$ and a simultaneous increase in $\Delta D_n$ were observed with each biopolymer deposition step, clearly indicating that the polyelectrolytes were gradually and sequentially deposited onto the surface of the QCMD sensor. During the rinses that followed the gelatin deposition, only small changes in $\Delta f_n/n$ and $\Delta D_n$ were observed, which showed that only a small fraction of the polyelectrolyte was desorbed on rinsing the film. In contrast, the pronounced increase in $\Delta f_n/n$ and decrease in $\Delta D_n$ observed during the rinsing steps following PGA adsorption indicated a greater loss of mass on rinsing the film. When the gelatin−PGA assembly approached the final 10th layer, the recorded total change in $\Delta f_n/n$ was $-380 \pm 70$ Hz ($\Delta f_3/3$), $-340 \pm 50$ Hz ($\Delta f_5/5$), and $-290 \pm 50$ Hz ($\Delta f_7/7$).

A different growth characteristic was observed when gelatin and PGA were assembled into multilayer films at 25 °C. The gelatin deposition resulted in smaller $\Delta f_n/n$ and $\Delta D_n$ shifts, indicating a lesser amount of gelatin being adsorbed in comparison to similar gelatin deposition steps performed at 30 and 37 °C. The subsequent rinses showed a small increase in $\Delta f_n/n$ accompanied by a decrease in $\Delta D_n$. The PGA depositions led to further and significant increases in $\Delta f_n/n$ and decreases in $\Delta D_n$, attributed to the fraction of the biopolymer being removed from the surface of the QCMD sensor. Nevertheless, overall, the trend for $\Delta f_n/n$ is negative, with a total frequency shift approaching $-70 \pm 10$ Hz ($\Delta f_3/3$), $-60 \pm 5$ Hz ($\Delta f_5/5$), and $-50 \pm 5$ Hz ($\Delta f_7/7$) at the 10th layer.

At temperatures of 37 and 30 °C the gelatin−PGA assembly resulted in the smallest total $\Delta f_n/n$, limited to $-27 \pm 3$ Hz at 37 °C, whereas at 30 °C, the total $\Delta f_n/n$ showed a small increase but was limited to $-33 \pm 5$ Hz. In both cases, a significant drop in frequency was observed for the first two layers, where the first layer was PLL (base layer) and the second layer was PGA. Although a large decrease in $\Delta f_n/n$ and an increase in $\Delta D_n$ were observed during the gelatin deposition step, indicating gelatin adsorption to the PGA layer, material was desorbed during the pH 7.0 and 5.0 rinsing steps that followed the gelatin deposition. This process was repeated for the subsequent three full deposition cycles with a cyclical frequency response superimposed on a slow increase frequency shift and dissipation.

A decrease in $\Delta f_n/n$ is a measure of the mass adsorption at each deposition step, and it is well-known that the QCMD response is sensitive to the viscoelastic properties of any mass coupled to the quartz crystal, including adsorbed biopolymers and water. The simplest model commonly used to analyze the QCMD data is the Sauerbrey equation. The $\Delta f_n/n$ values converted into hydrated mass using the Sauerbrey eq 2 indicated that the hydrated mass was greatest for the gelatin−PGA films assembled at 20 °C and that it decreased as the assembly temperature increased. The Sauerbrey model is, however, only valid in cases where the adsorbed films are predominantly elastic and there is negligible internal energy loss. Multilayer films tend to behave as viscoelastic rather than purely elastic films, and the viscous character is detected through the dissipation measurements. For elastic films, the $\Delta f_n/n$ values are the same for all overtones, whereas for viscoelastic films the $\Delta f_n/n$ values do not superimpose. Clearly the changes in dissipation observed during the gelatin−PGA film assembly indicates the formation of viscoelastic films, and

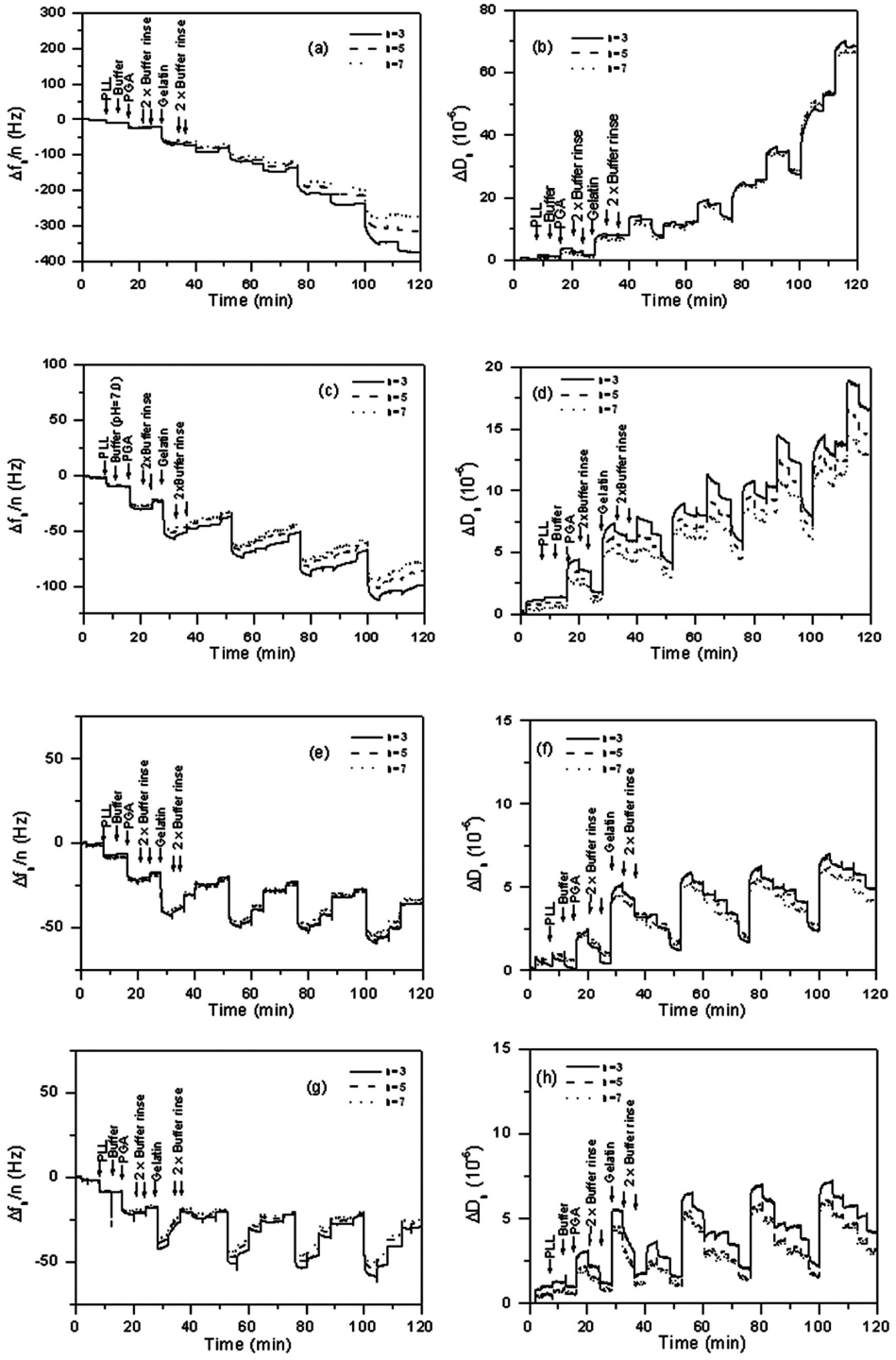


**Figure 1.** Temperature-dependent multilayer assembly of gelatin−PGA films. QCMD responses: (a) $\Delta f_n/n$ at 20 °C, (b) $\Delta D_n$ at 20 °C, (c) $\Delta f_n/n$ at 25 °C, (d) $\Delta D_n$ at 25 °C, (e) $\Delta f_n/n$ at 30 °C, (f) $\Delta D_n$ at 30 °C, (g) $\Delta f_n/n$ at 37 °C, and (h) $\Delta D_n$ at 37 °C.

thus the QCMD response was analyzed in more detail using the Voigt-based model.[47] In the Voigt model a multilayer is modeled as a homogeneous viscoelastic film, characterized by a shear viscosity, a shear modulus, an effective thickness, and density. The solution viscosity, $\eta_s$, and density, $\rho_s$, values for the films were taken to be 1 mPa·s and 1000 kg $m^{-3}$, respectively, and the effective film density $\rho_{eff}$ was assumed to be 1100 kg $m^{-3}$; the experimental data and best fit obtained using the Voigt-based model showed good agreement. Figure 2 indicates that the gelatin−PGA films formed at 20 °C show a continuous growth of the multilayer. In contrast, limited growth and a strong cyclical QCMD response were observed for the gelatin−PGA films formed at 30 and 37 °C, which resulted in the growth of relatively thin hydrated films.

The final hydrated masses calculated using both the Sauerbrey equation and the Voigt viscoelastic model are shown in Table 1 together with the viscoelastic properties of the gelatin−PGA films.

Comparison of the results shown in Table 1 shows that the highest hydrated mass films were deposited at 20 °C, and as the assembly temperature increased, lower hydrated mass films were formed. In terms of the viscoelastic properties, gelatin−PGA multilayer films assembled at 20 °C were characterized by the highest shear viscosity and shear

modulus values. Comparison of the hydrated masses calculated using the Voigt and Sauerbrey models showed that the hydrated mass estimate based on the Voigt model was larger than that calculated using the Sauerbrey equation by approximately 50 ± 10% and 35 ± 10% for films assembled at 20 and 25 °C, respectively. Figure 3 shows that the evolution of the hydrated mass, calculated using Sauerbrey eq 2 and the Voigt model, as a function of the number of layers for gelatin−PGA multilayers assembled at 20 and 25 °C, indicates that in both cases the hydrated mass was consistently underestimated by the Sauerbrey model at each deposition step. In the case of the assemblies formed at 30 and 37 °C the difference between the values calculated from the Voigt and Sauerbrey models was only 10%. The Voigt/Sauerbrey ratio, shown in Table 1, is therefore a measure of the extent to which the adsorbed layer has viscoelastic dissipative properties rather than the purely elastic response assumed in the Sauerbrey model.

A considerable amount of the published literature concerning gelatin has been focused on understanding the gelation mechanism for gelatin sols.[7−9] Previous studies have shown that the conformational changes of gelatin on cooling leads to association and the formation of thermoreversible gels. In an aqueous solution at temperatures above 35 °C, the gelatin chains adopt a random coil conformation. Upon cooling a partial regeneration of the collagen triple-helix structure occurs, in which hydrogen bonding is a dominant interaction,[6,7] leading to the formation of a gel. It is also well established that in solution gelatin is able to form electrostatic interactions.[12] The electrostatic interaction arises due to the presence of the charges on the polypeptide chain, and this type of interaction is strongly affected by the IEP of gelatin and the pH of the solution. The isoelectric point (IEP) of the gelatin used in this study occurs at pH 8.8, and thus at pH 5.0 the chains carry a net positive charge.[6] PGA has a $pK_a \sim 3.5$, and thus at pH 7.0 it was expected to be fully negatively charged.[48] Although the experimental conditions favored electrostatic interactions as the driving force during the gelatin−PGA assembly, the inhibited multilayer growth observed for layers formed at the temperature of 30 and 37 °C clearly indicated very weak electrostatic interactions between the polyelectrolytes used in this study. As previous studies by Caruso and co-workers have shown, in the case of electrostatically driven layer-by-layer assembly, there is a minimum charge density below which multilayer growth is not possible.[39] Continuous multilayer growth was observed for PGA with other polycations (e.g., poly-L-lysine) performed at 30 °C (data not shown). It is therefore believed that the charge density on gelatin at pH 5.0 at 30 and 37 °C appears to be lower than the critical charge density due to conformational changes (transition from triple helix, characterized by higher charge density to random coil characterized by lower charge density), thus resulting in limited multilayer assembly.

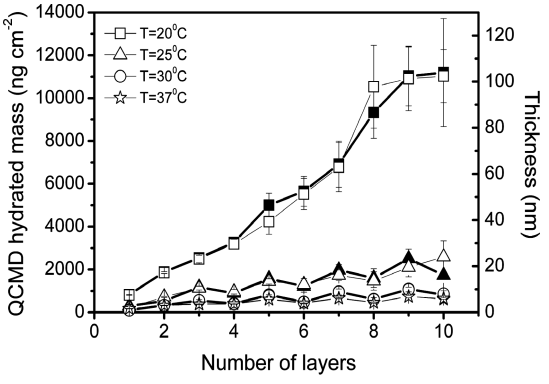


**Figure 2.** Temperature-dependent growth of gelatin−PGA multilayers. The evolution of the hydrated mass and thickness of the films calculated with the Voigt equation. Acoustic thickness is calculated from the hydrated mass assuming film density 1100 kg m$^{-3}$.

As the assembly temperature was decreased, an increase in the hydrated mass and thickness adsorbed during gelatin−PGA assembly was observed which implied the presence of an interaction that was not electrostatic in nature. The hydrogen bonds formed between the amino acid units cause the gelatin chains to adopt helix structures and consequently form physical gels as the temperature is decreased.[8,10] The coil−helix transition is predominantly intermolecular for gelatin solution concentrations above 0.5−1.0% (w/w). However, the gelatin solution used in this study had a very low concentration of 0.6 mg mL$^{-1}$, and thus it is believed that the coil−helix transition was predominantly intramolecular.[49]

An advantage of the QCMD technique is the ability to monitor viscoelastic properties through measurements of dissipation, as multilayer films are formed. It is known that elastic films have low dissipation values, whereas more viscoelastic structures exhibit higher dissipation values.[47] Overall, the significant changes in dissipation observed for the gelatin−PGA films assembled at 20 and 25 °C indicates the formation of viscoelastic films. A previous study conducted by Noel and co-workers reported that gelatin−pectin multilayer film assembly yielded highly hydrated films with a solid concentration reaching only 16% (w/w) after 8 layers.[14] The Noel and co-worker's study also reported a small decrease in dissipation during the pectin deposition steps, suggesting that the pectin was acting as a cross-linking agent in the network. In the present study, for the gelatin−PGA multilayers assembled at 20 °C, a significant increase in dissipation during both gelatin and PGA adsorption steps was observed, suggesting that both gelatin and PGA formed highly viscoelastic layers. However, a significant decrease in dissipation occurred during the rinse step with a pH 5.0 sodium phosphate solution that followed the PGA adsorption and led to a partial collapse of the PGA layer toward the surface and the formation of a denser film characterized by high shear viscosity and shear modulus values (Table 1). In the case of gelatin−PGA films assembled at 25 °C, the PGA deposition step led to a partial stripping effect due, we believe, to the formation of soluble complexes.[50] Regardless of the assembly temperature it was found, in agreement with

**Table 1. Properties of Layer-by-Layer Deposited Gelatin−PGA Films Estimated Using Sauerbrey and Voigt Models as a Function of Temperature**[a]

| assembly temperature (°C) | Sauerbrey mass (ng cm$^{-2}$) | Voigt mass (ng cm$^{-2}$) | Sauerbrey thickness (nm) | Voigt thickness (nm) | Voigt/Sauerbrey hydrated mass ratio | shear viscosity (mPa·s) | shear modulus (MPa) |
|---|---|---|---|---|---|---|---|
| 20 | 7100 ± 1200 | 11300 ± 2700 | 65 ± 12 | 100 ± 25 | 1.6 | 3.9 | 0.280 |
| 25 | 1900 ± 600 | 2700 ± 900 | 17 ± 6 | 24 ± 7 | 1.4 | 2.4 | 0.176 |
| 30 | 750 ± 150 | 820 ± 200 | 7 ± 1.5 | 8 ± 2 | 1.1 | 1.5 | 0.025 |
| 37 | 550 ± 40 | 600 ± 100 | 5 ± 0.5 | 6 ± 1 | 1.1 | 1.4 | 0.016 |

[a] Film thicknesses calculated from hydrated masses by assuming $\rho_{eff}$ is 1100 kg m$^{-3}$.

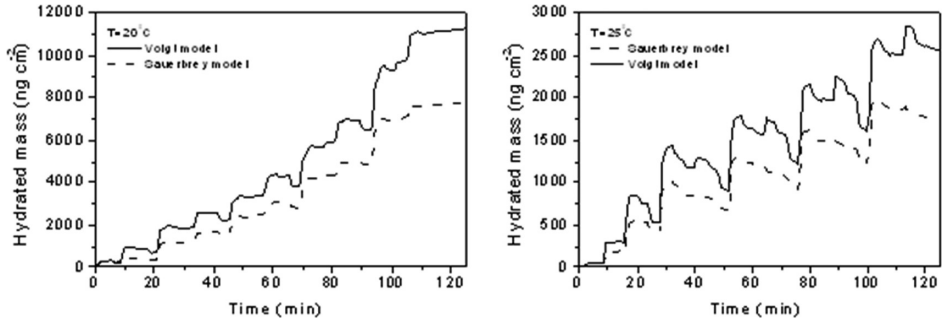


**Figure 3.** Evolution of the hydrated mass during the assembly of gelatin−PGA films at 20 and 25 °C, calculated using the Sauerbrey and Voigt models.

reports by Notley co-workers that there were fundamental differences in the gelatin−PGA multilayer structures which depended upon the nature of the polymer being deposited as the outmost layer.[51] In the present case for the gelatin−PGA films the formation of multilayers with higher shear viscosity values (4.1 and 2.8 mPa·s at 20 and 25 °C, respectively) was observed when gelatin was the outermost layer (ninth layer), whereas the "stiffening" of the multilayer was caused by the deposition of PGA as the outermost layer (3.9 and 2.36 mPa·s at 20 and 25 °C, respectively).

The results showed that the assembly temperature played a crucial role in gelatin−PGA assembly. The conformational changes and the formation of hydrogen bonds between the gelatin chains and PGA were temperature-dependent. The lower the temperature, the greater the quantity of hydrogen bonds formed and therefore the more mass adsorbed, enabling the use of temperature to tune the properties of the gelatin−PGA multilayer films.

Changes in the viscoelastic properties of the gelatin−PGA films with temperature were also observed using AFM. Figures 4a,c,f show "stiffness" maps, and corresponding topographical images (Figures 4b,d,e) of a 25 $\mu$m area of a gelatin−PGA film captured at 20, 30, and 37 °C, respectively. Gelatin−PGA films imaged at 20 °C typically exhibited heterogeneous topography. The tall features seen in Figures 4a,b are believed to be aggregates of gelatin. At 30 °C, these aggregates appeared smaller in size (Figures 4c,d), presumably due to softening and partial melting at the higher temperature. The topographical image of the gelatin−PGA film obtained at 37 °C (at which gelatin will be melted and adopts the random coil conformation, Figures 4e,f) shows the disappearance of the large aggregates and the formation of a more uniform structure. The sudden color change in Figure 4e shown near the bottom of the image was due to the tip picking up some of the sample material during imaging. Analysis of the stiffness maps provided crucial information about the viscoelastic properties of the gelatin−PGA films. The force maps were obtained using a colloidal glass sphere attached to the cantilever in place of the normal AFM tip to allow better detection of the softness of the gelatin−PGA films, as a standard sharp tip can often simply push straight through a soft sample onto the underlying mica. To validate this approach, we included a control data set showing "stiffness" and topography maps (Figures 4g,h) obtained with the colloid probe tip probing a bare glass slide. The much lower value and range of both data sets in Figures 4g,h compared to Figures 4a−f confirm that the data obtained on the gelatin−PGA sample comes principally from deformation of the films. The "stiffness" maps seen in Figures 4a,c,f display the relative mechanical properties of the gelatin−PGA film by quantifying the inverse optical lever sensitivity (INVOLS), using a "cold−hot" color table to represent the data. In this scheme data values are represented as blue colors at the low end, through red to yellow at the high end. High values in this data correspond to softer regions of the sample surface. At 20 °C the stiffness map (Figure 4a) reveals that there is considerable heterogeneity within the film, with the tall gelatin aggregates seen in the corresponding topography data (Figure 4b) appearing significantly softer than the rest of the layer. As the temperature is raised to 30 °C (Figures 4c,d), the heterogeneity in the mechanical properties of the film appeared to reduce significantly as a consequence of the entire film becoming softer, as the gelatin partially melted. At the highest temperature studied (37 °C, Figures 4e,f) a dramatic change is observed, the aggregates disappear from the topography image, and the film becomes noticeably harder and more homogeneous. Taken together with the QCMD data, which show limited multilayer growth at 37 °C (Figures 1g,h), we interpreted this as evidence that the gelatin was being lost from the film, leaving it composed principally of PLL and PGA.

QCMD was then used to investigate of the response of gelatin−PGA assemblies to changes in temperature, pH, and ionic strength ionic strength. Because of the limited multilayer growth observed for gelatin−PGA films at 30 and 37 °C (Figures 1 and 2), the environmental response study was restricted to gelatin−PGA multilayers that were assembled only at 20 and 25 °C.

**Temperature Effect.** Figure 4 shows the effect of temperature on gelatin−PGA multilayer films. The temperature was increased in 4 °C increments, starting from the assembly temperatures of 20 or 25 °C, to 37 °C, at which gelatin helices are expected to be fully melted and the chains adopt a random coil structure.[7]

Significant increases in $\Delta f_n/n$ and decreases in $\Delta D_n$ were observed as the temperature was gradually incremented from 20 to 37 °C (Figures 5a,b). The greatest changes in both $\Delta f_n/n$ and $\Delta D_n$ occurred within the temperature range 24−28 °C. The $\Delta f_n/n$ values increased by approximately 200 Hz ($\Delta f_3/3$), 120 Hz ($\Delta f_5/5$), and 90 Hz ($\Delta f_7/7$) while over the same temperature range the $\Delta D_n$ values decreased by $\sim 60 \times 10^{-6}$ for all overtones. As the temperature was increased to 32 °C, almost 90% of the mass from the original gelatin−PGA film was released from the surface. Finally, at the 37 °C we observed a positive value for $\Delta f_n/n$ and negative value for $\Delta D_n$, respectively. The subsequent gradual decrease of temperature back to 20 °C resulted in final values of $\Delta f_n/n = -70$ Hz and $\Delta D_n = 20 \times 10^{-6}$, respectively. Consequently, the overall result of the temperature modulation was an increase in $\Delta f_n/n$ by ~400 Hz and a decrease in $\Delta D_n$ by $\sim 100 \times 10^{-6}$.

The gelatin−PGA multilayer films formed at 25 °C showed similar behavior to those formed at 20 °C (Figures 5c,d). Because of the overall smaller amount of mass adsorbed at 25 °C, when compared to that adsorbed at 20 °C, the $\Delta f_n/n$ shifts observed were proportionally smaller; however, the overall trend was the same. As a result of

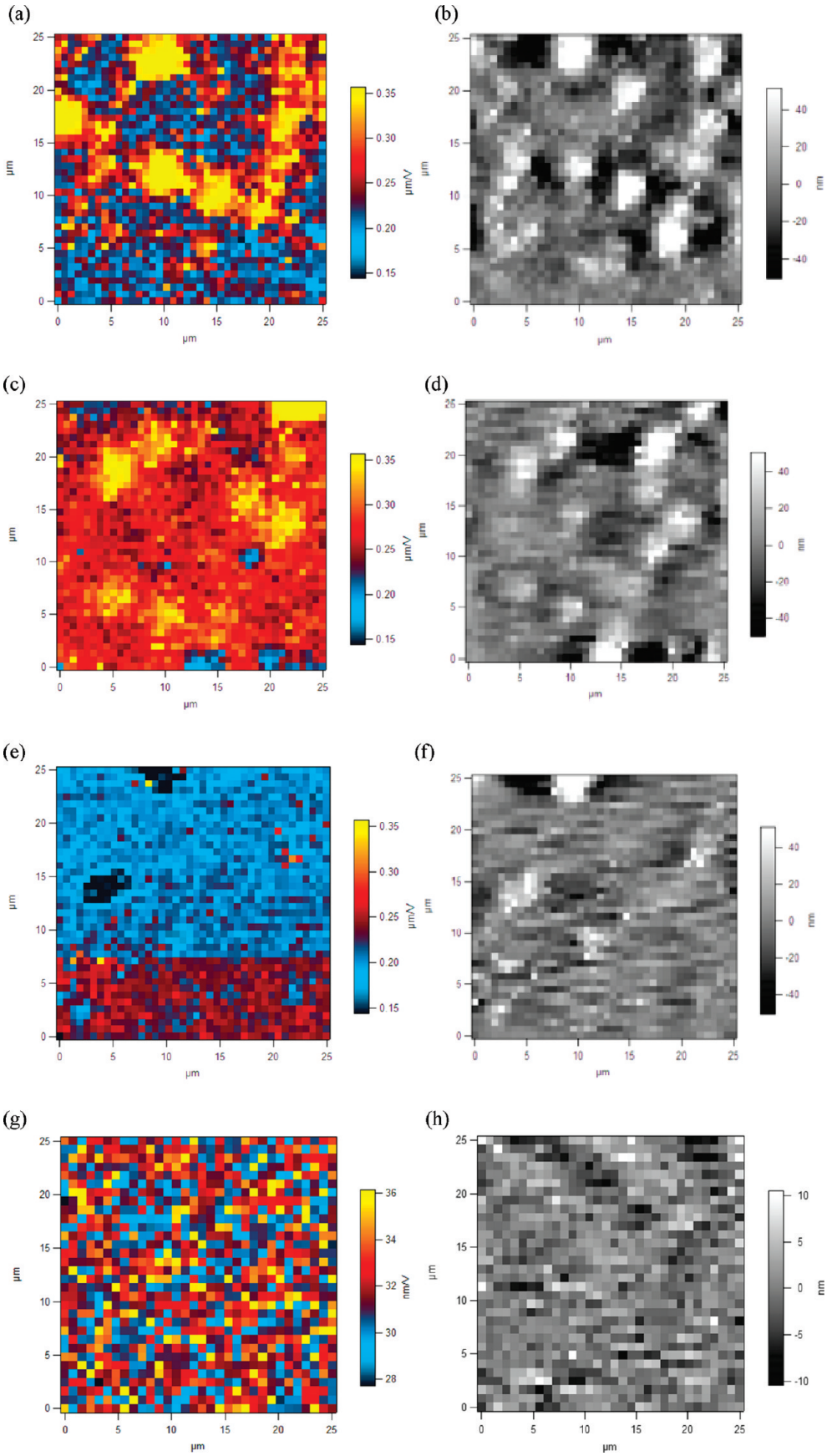


**Figure 4.** Force ("stiffness") maps of a 25 $\mu$m area of a gelatin−PGA film captured at (a) 20, (c) 30, and (e) 37 °C and corresponding topographical images of a 25 $\mu$m area of a gelatin−PGA film captured at (b) 20, (d) 30, and (f) 37 °C; (g) force ("stiffness") map of a 25 $\mu$m area of a glass slide and (h) a corresponding topographical image of a 25 $\mu$m area.

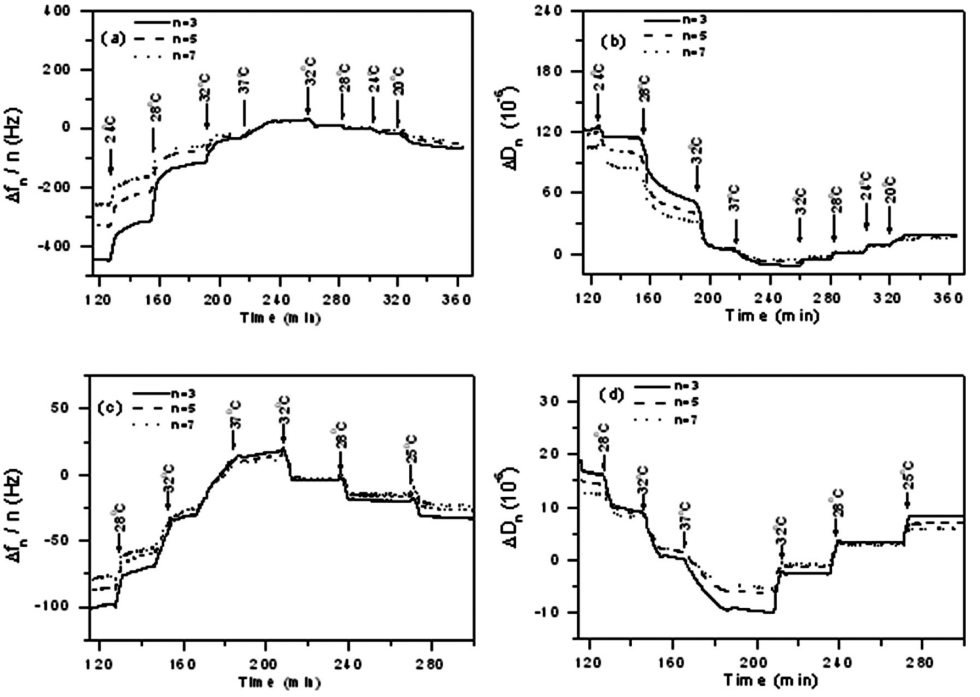


**Figure 5.** QCMD responses in $\Delta f_n/n$ and $\Delta D_n$ to changes in temperature for gelatin−PGA multilayer films: (a) $\Delta f_n/n$ and (b) $\Delta D_n$ for gelatin−PGA multilayer films formed at 20 °C and (c) $\Delta f_n/n$ and (d) $\Delta D_n$ for gelatin−PGA multilayer films formed at 25 °C.

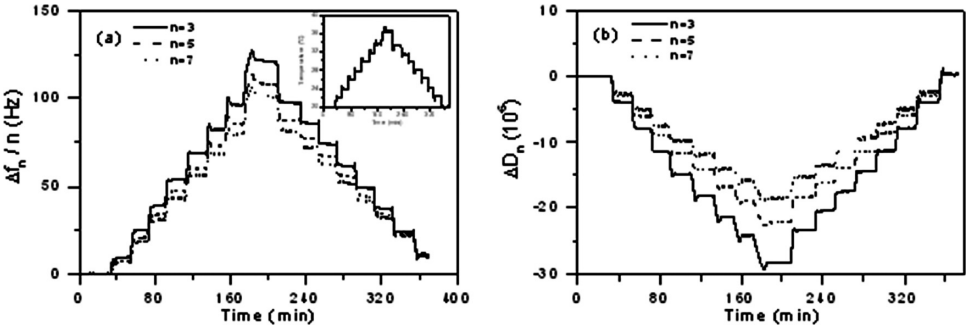


**Figure 6.** Effect of temperature on (a) $\Delta f_n/n$ and (b) $\Delta D_n$ for a $SiO_2$ QCMD sensor. Inset shows the temperature cycle.

temperature modulation, we observed an increase in $\Delta f_n/n$ of ~75 Hz and a decrease in $\Delta D_n$ by $\sim 10 \times 10^{-6}$.

The positive values of $\Delta f_n/n$ and the negative values of $\Delta D_n$ observed at 37 °C reflect that the temperature affects the quartz crystal microbalance in addition to the material adjacent to the quartz crystal surface. In order to extract information related purely to the effect of temperature on film structure, we examined the temperature effect on the oscillation of bare silica-based QCMD crystals. Figure 6 shows the results of a control experiment in which the bare QCMD crystal was submitted to the same temperature history as in the temperature responsiveness experiment (see the inset in Figure 6a), and it shows that over the temperature range 20−37 °C there is a largely reversible change in $\Delta f$. Each temperature increment led to the similar changes in $\Delta f_n/n$ and $\Delta D_n$, and overall, the change in temperature from 20 to 37 °C caused a total increase of $\Delta f_n/n$ by ~110 ± 10 Hz and a total decrease in $\Delta D_n$ of $(25 \pm 5) \times 10^{-6}$.

The temperature-related changes in $\Delta f_n/n$ and $\Delta D_n$ observed for gelatin−PGA multilayer films assembled at 20 °C were much greater than those observed for the silica-based QCMD sensors, indicating that structural changes occurred within the gelatin−PGA films.

In order to estimate the temperature-dependent structural changes occurring to the gelatin−PGA films, we subtracted the shifts in $\Delta f_n/n$ and $\Delta D_n$ caused by the temperature gradient alone, from the total values of $\Delta f_n/n$ and $\Delta D_n$ obtained at each temperature, respectively. The results showed that the gelatin−PGA film assembled at 20 °C was almost completely washed away as the temperature reached 32 °C (Figure 7), leaving, as we believe the first two layers of PLL and PGA intact, with some gelatin still bound to these two layers. With a total loss of hydrated mass of 90%, this corresponds to ~1000 ng $cm^{-2}$ of the hydrated mass remaining at the surface. The hydrated mass of the first two layers during the assembly process was estimated to be 520 ± 100 ng $cm^{-2}$, while the deposition of the third (gelatin) layer led to a total hydrated mass of 1630 ± 250 ng $cm^{-2}$, which clearly indicated that a structure less than a three-layer film remained at the surface after the gelatin−PGA film was subjected to the temperature challenge. In order to confirm the hypothesis that the first two layers were unaffected during the temperature cycle, we also performed an additional experiment (data not shown), in which a 10-layer film consisting of only PLL and PGA was subjected to the same temperature challenge as the gelatin−PGA films under investigation, and as expected, the PLL−PGA multilayer film remained unchanged.

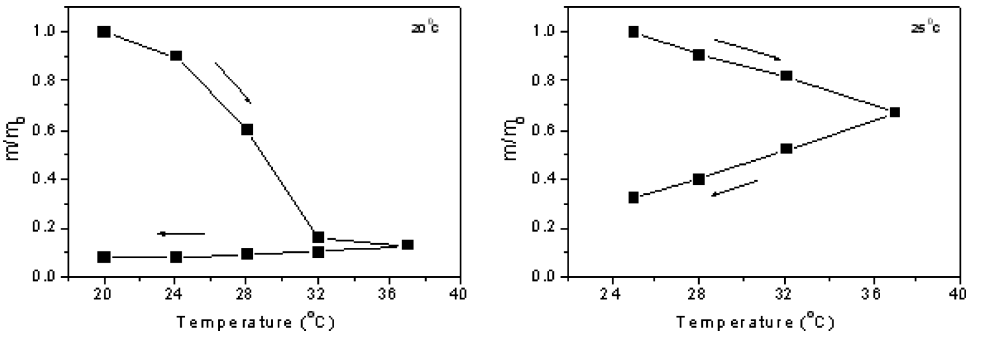


**Figure 7.** Influence of temperature on the normalized hydrated mass of gelatin−PGA multilayer films assembled at 20 and 25 °C (arrows indicate the direction of the temperature cycling steps).

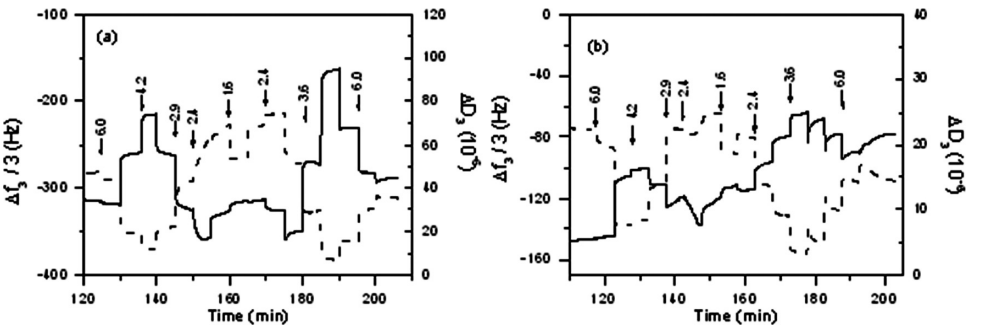


**Figure 8.** QCMD responses $\Delta f_3/3$ (—) and $\Delta D_3$ (- - -) to changes in pH for gelatin−PGA assemblies formed at (a) 20 °C and (b) 25 °C.

The gelatin−PGA film fabricated at 25 °C exhibited gradual disassembly as the temperature was first elevated to 37 °C and then decreased back to 25 °C (Figure 7b). The temperature cycle resulted in a total loss of 70% of the hydrated mass for the gelatin−PGA film assembled at 25 °C. Although gelatin−PGA films assembled at 25 °C showed a lower degree of disassembly compared to similar films assembled at 20 °C, the mass remaining at the surface was, however, only 600 ng $cm^{-2}$, and this clearly suggested that only the first two layers were unaffected by the temperature cycle.

Generally, elevated temperature can lead to changes in polymer−solution interactions which can result in polyelectrolytes adopting conformations that are normaly unfavorable at lower temperatures.[52] Because of the higher mobility of polyelectrolytes at higher temperatures, the structural integrity of the film may only withstand certain temperatures. If the hydrogen bonding is weakened as temperature is increased,[53] as has been proven, it is therefore not surprising that, at higher temperatures, the hydrogen bonds among the molecules break and lead to disassembly of the gelatin−PGA films. Additionally, the partially restored collagen triple-helix structure, which gelatin adopts at room temperature, will melt with increasing temperature. Although it has been shown that cross-linking between amine and carboxylic groups is favored at higher temperatures, it is only true for the first two layers, which were assembled via electrostatic interaction and which remain unaffected by the changes in temperature.[54] In terms of interactions between PGA and gelatin, this type of interaction did not occur to such a significant extent as to prevent disintegration of the films when the temperature was raised to 37 °C.

**pH Effect.** pH responses were studied within the range 1.6−7.0. Figure 8 shows the QCMD response from gelatin−PGA assemblies to a decrease in pH from 7.0 down to 1.6 and then an increase in pH back to 7.0. It is noticeable that the gelatin−PGA multilayer films formed at 20 and 25 °C responded to pH changes in a broadly similar manner. The variation of pH led to alternate increases and decreases in $\Delta f_n/n$. The initial decrease in pH from 7.0 to 4.2 led to an increase in $\Delta f_n/n$, which passed through a maximum and then decreased again, as the pH dropped to 2.4. The $\Delta f_n/n$ values then increased again as the pH was lowered to 1.6. This was then followed by alternate decreases and increases in $\Delta f_n/n$ as the pH was progressively returned to neutral. The behavior of the measured $\Delta D_n$, mirrored that seen with $\Delta f_n/n$: increases and decreases in $\Delta D_n$ corresponded to decreases and increases in $\Delta f_n/n$. An important observation was that, after pH cycling, gelatin−PGA films assembled at 20 °C returned almost completely to their original hydrated mass, as measured prior to changing the pH of the external solution. However, the gelatin−PGA assembly formed at 25 °C showed irreversible changes: overall after completion of the pH cycle the $\Delta f_n/n$ value increased by ~70 Hz and $\Delta D_n$ decreased by $\sim 8 \times 10^{-6}$.

There is a substantial amount of published work which describes how the properties of multilayer films composed of weak polyelectrolytes are responsive to pH. An additional characteristic of these multilayer films is that a pH-triggered restructuring leading to partial or full disassembly is likely to occur; this requirement is essential when considering controlled and site-specific delivery applications.[1,31,55,56]

Although pH responsiveness is typically associated with the multilayers formed through electrostatic interactions, Granick and Sukhishvili[32,38] fabricated pH-responsive multilayer films assembled via hydrogen bond interactions. They proposed that the critical pH for film decomposition is controlled by the balance of internal ionization, mainly the fraction of carboxylic groups remaining within the film. Caruso et al.[39] showed that pH-induced decomposition of hydrogen-bonded multilayer films is strongly dependent on the hydrogen-bonded layer thickness.

This study has shown that gelatin−PGA multilayer films fabricated at 20 °C undergo essentially reversible alternate

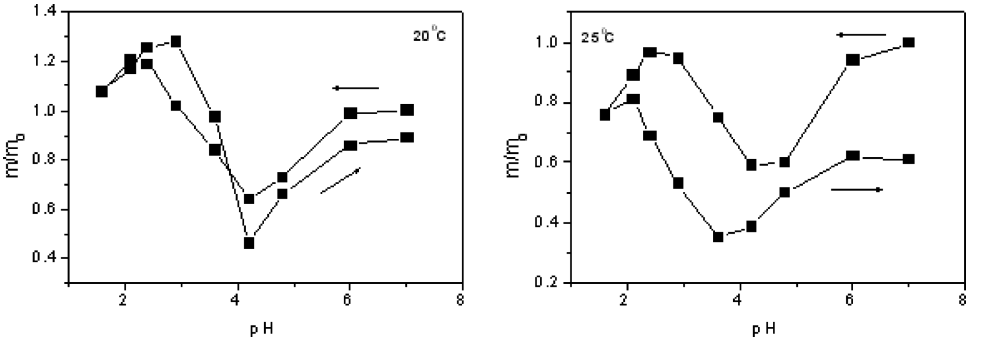


**Figure 9.** Influence of pH on hydrated mass of gelatin−PGA multilayer films assembled at 20 and 25 °C (arrows indicate the order of the pH cycling steps).

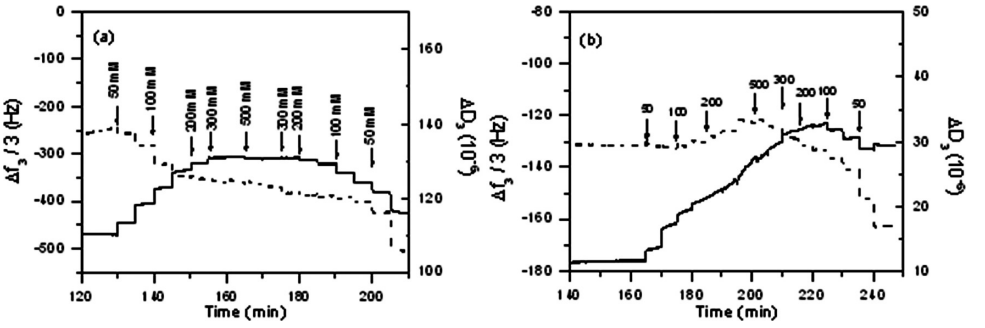


**Figure 10.** QCMD response ($\Delta f_3/3$ (—) and $\Delta D_3$ (- - -) data) of gelatin−PGA assemblies formed at (a) 20 °C and (b) 25 °C to changes in NaCl concentration. Although measurements of the quartz crystal oscillator frequency and dissipation were made at three overtones, for reasons of clarity only results obtained for the third overtone are shown.

swelling and deswelling changes in response to changes in pH (Figure 9). The variation of external pH resulted in changes in charge density within the gelatin−PGA films, which consequently led to significant structural alterations within the films. It has been previously reported that the p$K_a$ of PGA is ~3.5, which means that at pH 7.0 the PGA will be fully charged.[48] The IEP of the gelatin used in this study occurs at 8.8, and at pH 5.0 the gelatin will carry a net positive charge. In physicochemical terms, lowering the pH causes protonation of the carboxylate groups of the PGA and gelatin, thus removing their charge, affecting the electrostatic interactions within the multilayer. Therefore, the initial decrease of pH led to the reduction of the repulsive force between like charges on PGA backbone by protonation of $COO^-$ groups of the anhydrogalacturonic acid residues. Decrease of pH also led to an increase in the net positive charge of the gelatin chains. Because of the increase of electrostatic repulsion between the positively charged segments, the gelatin chains adopted a stretched conformation. In addition to the conformational changes of the individual components, the electrostatic interaction between the gelatin and PGA will strengthen over the pH range for which the charge on the gelatin increases but the PGA does not significantly decrease. A combination of these factors caused the film to shrink. However, a further decrease of pH to below the p$K_a$ of PGA led to the swelling effect caused, as we propose, by a decrease in the strength of interactions restraining swelling due to weaker gelatin−PGA interactions. Additionally, the continuous protonation of $COO^-$ groups as the pH was decreased caused the PGA chains to adopt a conformation rich in loops and trains, which consequently led to a swelling of the multilayers. An increase of pH back to neutral values would lead to an increase in charge density as the COOH groups become charged again. The gelatin−PGA films assembled at 20 °C did not show pronounced pH-triggered decomposition, as the total estimated hydrated mass loss was only 10%. This behavior is in agreement with the work of Noel and co-workers on gelatin−pectin multilayers, who also reported no disassembly pH-induced event.[14] The great stability of the film was attributed to a significant number of hydrogen bonds formed between the biopolymers, which seemed to be unaffected by the pH variation. Although the assembly of gelatin−PGA systems at 25 °C is also driven by the formation of hydrogen bonds, in this case the interactions between the polymers are weaker compared to gelatin−PGA assemblies formed at 20 °C, and therefore the pH cycling resulted in partial film dissolution. Gelatin−PGA multilayer films assembled at 25 °C showed the same (de)swelling behavior in response to pH, as for similar films assembled at 20 °C (Figure 9). However, in this case the total loss of hydrated mass was estimated to be 40%, and the remaining film was characterized by a lower shear viscosity (1.8 mPa·s) and shear modulus (0.140 MPa).

**Salt Effect.** We have examined the effect of ionic strength on gelatin−PGA multilayer films assembled at 20 and 25 °C. Figure 10 shows the response of gelatin−PGA films to changes in ionic strength over the range 30−500 mM NaCl. For a gelatin−PGA multilayer film assembled at 20 °C, a gradual increase of ionic strength from 30 to 300 mM resulted in a significant increase in $\Delta f_n/n$ and a less pronounced decrease in $\Delta D_n$. The total shifts of $\Delta f_n/n$ and $\Delta D_n$ observed were approximately $105 \pm 15$ Hz and $(20 \pm 5) \times 10^{-6}$, respectively. A further increase in ionic strength resulted in no additional changes in both $\Delta f_n/n$ and $\Delta D_n$. A decrease of ionic strength back to 30 mM resulted in an increase in $\Delta f_n/n$ with minor changes in $\Delta D_n$, indicating partial reversibility (Figure 10a).

The gelatin−PGA multilayer films formed at 25 °C showed a slightly different response to ionic strength in comparison to gelatin−PGA film assembled at 20 °C

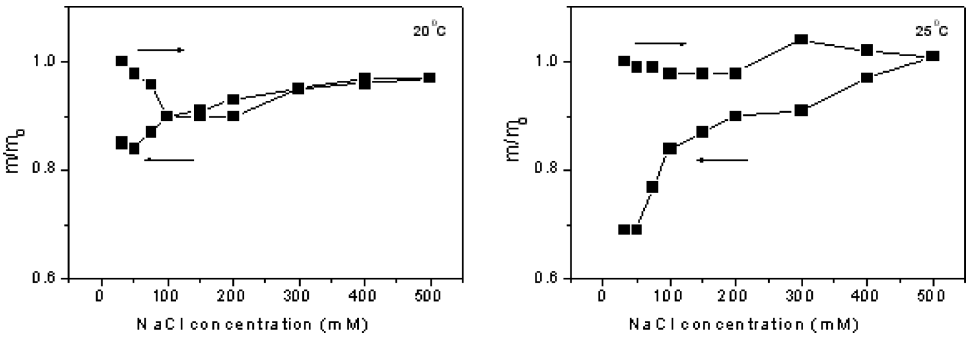


**Figure 11.** Influence of NaCl concentration on hydrated mass of gelatin−PGA multilayer films assembled at 20 and 25 °C (arrows indicate the direction of the salt concentration cycling stages).

(Figure 10b). In this case, the gradual increase in ionic strength from 30 to 500 mM NaCl led to an increase in $\Delta f_n/n$ of $\sim 30 \pm 5$ Hz, whereas $\Delta D_n$ increased by $\sim(3 \pm 2) \times 10^{-6}$. Gradual decrease of ionic strength from 500 to 150 mM resulted in a further increase in $\Delta f_n/n$. This was followed by a decrease of $\Delta f_n/n$, as the ionic strength was lowered back to 30 mM. The dissipation measurements revealed a continuous decrease in $\Delta D_n$ values as the ionic strength was gradually lowered back to 30 mM.

Irrespective of whether the gelatin−PGA multilayer assemblies were prepared at 20 or 25 °C, in both cases the response of the films to changes in ionic strength resulted in irreversible changes within the film structure, as both the frequency and dissipation parameters did not return to their original values prior to performing the salt response experiment.

The swelling profile of gelatin−PGA films assembled at 20 °C indicated that overall the films were not strongly affected by the changes in ionic strength (Figure 11). The increase in ionic strength led initially to shrinkage of the films. Kamiyama and Israelachvili[12] postulated that, below the IEP and at low salt concentrations, gelatin molecules are believed to be expanded due to electrostatic repulsions between the positively charged segments. Thus, increasing the ionic strength will screen the charge present on free functional groups of the biopolymers within the film. This will cause the chains to collapse resulting in a reduced thickness of the film. However, the shrinkage of the gelatin−PGA multilayer films reached a maximum at 100 mM NaCl. A further increase of ionic strength is considered to cause the osmotic pressure within the multilayer film to increase leading to the opposite effect of swelling. This phenomenon is typical of the swelling behavior observed for polyampholyte networks with an intermediate net charge.[26] When the salt concentration was decreased back to 30 mM NaCl, a great degree of reversibility was observed in the swelling behavior of the gelatin−PGA films. Bearing in mind that hydrogen bond formation was driving the assembly of the gelatin−PGA multilayer films, we postulate that the observed small degree of disassembly of the films (15% mass loss) was mainly due to water being expelled from the film. This was confirmed by the significant decrease in dissipation; a decrease of shear viscosity from 3.90 to 3.1 mPa·s and an increase in shear modulus from 0.290 to 0.340 MPa, which indicates formation of a less viscous and more rigid film.

Gelatin−PGA films assembled at 25 °C showed small changes in $m/m_0$ ratio in response to increasing the ionic strength. Likewise, the gelatin−PGA films assembled at 20 °C, and the films assembled at 25 °C exhibited an initial shrinkage followed by a swelling behavior. However, as the NaCl concentration was decreased, a significant dissolution of the film was observed. An increase of the shear viscosity and shear modulus to 2.5 mPa·s and 0.210 MPa, respectively, suggested that the total observed loss of hydrated mass of 30% for a gelatin−PGA assembly formed at 25 °C corresponded to the loss of the trapped water and polymer which formed the uppermost layers.[25]

The significant change in response to changes of salt concentration was related to the temperature-dependent conformational change of gelatin, which greatly influenced the interactions between the gelatin and PGA layers within the multilayers. The results of the temperature-dependent assembly showing a significantly different growth of hydrated mass during the assembly of gelatin−PGA multilayers at 20 and 25 °C clearly indicated that the interactions between gelatin and the PGA layer were considerably weaker for the film fabricated at 25 °C. Because of the temperature-dependent conformational change of gelatin, it gradually underwent a transition from the triple helix to a random coil conformation when the gelatin finally melted at temperature above 35 °C. The conformational changes started occurring as the temperature was elevated above 20 °C, progressively breaking the interactions within the gelatin−PGA films. Additionally, as already shown, the conformational changes also influenced the charge density of gelatin. Diffusion of the salt ions in and out of the film during the ionic strength challenge led to an increase or decrease of the repulsive and attractive electrostatic interactions between the layers.[38,57] This caused further conformational changes, which indirectly led to additional weakening of the interactions between the gelatin and PGA layers. This therefore resulted in an overall higher degree of dissolution of the gelatin−PGA multilayer fabricated at 25 °C in response to the salt challenge.

## Conclusions

Gelatin−PGA multilayer films were prepared at different assembly temperatures ranging from 20 to 37 °C using the layer-by-layer approach. These multilayer films were then subjected to changes in ionic strength, pH, and temperature in order to study the stability of the gelatin−PGA films to environmental stresses. The results showed that the assembly temperature was crucial to gelatin−PGA assembly. In terms of hydrated mass, the highest amount adsorbed and consequently the thickest gelatin−PGA assemblies were formed at 20 °C, whereas limited growth was observed for gelatin−PGA films assembled at 37 °C. For the experimental conditions used in the present study gelatin and PGA are respectively positively and negatively charged, creating favorable conditions for electrostatic interactions to drive the layer-by-layer assembly process. Despite this the present study showed that the driving force for the gelatin−PGA assembly was hydrogen bonding within the films. The stability of

assembled gelatin−PGA multilayer films to various environmental stresses was found to be significantly influenced by the changes in temperature. At low temperatures the behavior of gelatin was dominated by helix formation and association through hydrogen bonding. Raising the temperature promotes melting of the helix, disruption of the multilayer network, and disassembly of the films. This study also showed that gelatin−PGA multilayer films fabricated at 20 °C undergo almost completely reversible alternate (de)swelling changes in response to changes in pH and ionic strength. In contrast, gelatin−PGA multilayer films formed at 25 °C showed a partial decomposition when exposed to various pH and salt concentrations. In summary, this study shows that various gelatin−PGA multilayer structures can be fabricated and that the properties can be manipulated to give desired responsiveness to environmental change.

**Acknowledgment.** The UK Biotechnology and Biological Sciences Research Council supported this research from the Institute Strategic Programme Grant and through the award of responsive mode grants (BBC5044781, BBE0131711, and BBE0110041). We thank Professor Victor J. Morris and Timothy R. Noel for their support and very useful comments.

## References and Notes

(1) Pargaonkar, N.; Lvov, Y. M.; Li, N.; Steenekamp, J. H.; de Villiers, M. M. *Pharm. Res.* **2005**, *22* (5), 826–835.
(2) Tharanathan, R. N. *Trends Food Sci. Technol.* **2003**, *14* (3), 71–78.
(3) Tabata, Y.; Ikada, Y. *Adv. Drug Delivery Rev.* **1998**, *31* (3), 287–301.
(4) Golumbek, P. T.; Azhari, R.; Jaffee, E. M.; Levitsky, H. I.; Lazenby, A.; Leong, K.; Pardoll, D. M. *Cancer Res.* **1993**, *53* (24), 5841–5844.
(5) Harrison, M.; Hills, B. P. *Int. J. Food Sci. Technol.* **1996**, *31* (2), 167–176.
(6) Djabourov, M. *Polym. Int.* **1991**, *25* (3), 135–143.
(7) Djabourov, M.; Leblond, J.; Papon, P. *J. Phys.* (*Paris*) **1988**, *49* (2), 319–332.
(8) Harrington, W. F.; Rao, N. V. *Biochemistry* **1970**, *9* (19), 3714–3724.
(9) Mackie, A. R.; Gunning, A. P.; Ridout, M. J.; Morris, V. J. *Biopolymers* **1998**, *46* (4), 245–252.
(10) Joly-Duhamel, C.; Hellio, D.; Djabourov, M. *Langmuir* **2002**, *18* (19), 7208–7217.
(11) Curme, H. G.; Natale, C. C. *J. Phys. Chem.* **1964**, *68*, 3009–3016.
(12) Kamiyama, Y.; Israelachvili, J. *Macromolecules* **1992**, *25* (19), 5081–5088.
(13) Lin, Y.; Wang, L. L.; Zhang, P. B.; Wang, X.; Chen, X. S.; Jing, X. B.; Su, Z. H. *Acta Biomater.* **2006**, *2* (2), 155–164.
(14) Noel, T. R.; Krzeminski, A.; Moffat, J.; Parker, R.; Wellner, N.; Ring, S. G. *Carbohydr. Polym.* **2007**, *70*, 393–405.
(15) Decher, G. *Science* **1997**, *277* (5330), 1232–1237.
(16) Halthur, T. J.; Claesson, P. M.; Elofsson, U. M. *J. Am. Chem. Soc.* **2004**, *126* (51), 17009–17015.
(17) Hoogeveen, N. G.; Stuart, M. A. C.; Fleer, G. J.; Bohmer, M. R. *Langmuir* **1996**, *12* (15), 3675–3681.
(18) Izumrudov, V.; Sukhishvili, S. A. *Langmuir* **2003**, *19* (13), 5188–5191.
(19) Lavalle, P.; Gergely, C.; Cuisinier, F. J. G.; Decher, G.; Schaaf, P.; Voegel, J. C.; Picart, C. *Macromolecules* **2002**, *35* (11), 4458–4465.
(20) Lvov, Y.; Ariga, K.; Kunitake, T. *Chem. Lett.* **1994**, *12*, 2323–2326.
(21) Muller, M.; Kessler, B.; Houbenov, N.; Bohata, K.; Pientka, Z.; Brynda, E. *Biomacromolecules* **2006**, *7* (4), 1285–1294.
(22) Shiratori, S. S.; Rubner, M. F. *Macromolecules* **2000**, *33* (11), 4213–4219.
(23) Zhang, J.; Senger, B.; Vautier, D.; Picart, C.; Schaaf, P.; Voegel, J. C.; Lavalle, P. *Biomaterials* **2005**, *26* (16), 3353–3361.
(24) Dubas, S. T.; Schlenoff, J. B. *Macromolecules* **2001**, *34* (11), 3736–3740.
(25) Krzeminski, A.; Marudova, M.; Moffat, J.; Noel, T. R.; Parker, R.; Wellner, N.; Ring, S. G. *Biomacromolecules* **2006**, *7* (2), 498–506.
(26) Ogawa, Y.; Ogawa, K.; Kokufuta, E. *Langmuir* **2004**, *20* (7), 2546–2552.
(27) Picart, C.; Lavalle, P.; Hubert, P.; Cuisinier, F. J. G.; Decher, G.; Schaaf, P.; Voegel, J. C. *Langmuir* **2001**, *17* (23), 7414–7424.
(28) Schneider, A.; Picart, C.; Senger, B.; Schaaf, P.; Voegel, J. C.; Frisch, B. *Langmuir* **2007**, *23* (5), 2655–2662.
(29) Mendelsohn, J. D.; Barrett, C. J.; Chan, V. V.; Pal, A. J.; Mayes, A. M.; Rubner, M. F. *Langmuir* **2000**, *16* (11), 5017–5023.
(30) Moffat, J.; Noel, T. R.; Parker, R.; Wellner, N.; Ring, S. G. *Carbohydr. Polym.* **2007**, *70* (4), 422–429.
(31) Sukhorukov, G. B.; Antipov, A. A.; Voigt, A.; Donath, E.; Mohwald, H. *Macromol. Rapid Commun.* **2001**, *22* (1), 44–46.
(32) Kharlampieva, E.; Sukhishvili, S. A. *Macromolecules* **2003**, *36* (26), 9950–9956.
(33) Boulmedais, F.; Bozonnet, M.; Schwinte, P.; Voegel, J. C.; Schaaf, P. *Langmuir* **2003**, *19* (23), 9873–9882.
(34) Erel-Unal, I.; Sukhishvili, S. A. *Macromolecules* **2008**, *41* (22), 8737–8744.
(35) Kozlovskaya, V.; Sukhishvili, S. A. *Macromolecules* **2006**, *39* (16), 5569–5572.
(36) Kozlovskaya, V.; Sukhishvili, S. A. *Macromolecules* **2006**, *39* (18), 6191–6199.
(37) Stockton, W. B.; Rubner, M. F. *Macromolecules* **1997**, *30* (9), 2717–2725.
(38) Sukhishvili, S. A.; Granick, S. *Macromolecules* **2002**, *35* (1), 301–310.
(39) Cho, J.; Caruso, F. *Macromolecules* **2003**, *36* (8), 2845–2851.
(40) Burke, S. E.; Barrett, C. J. *Biomacromolecules* **2003**, *4* (6), 1773–1783.
(41) Sauerbrey, G. *Z. Phys.* **1959**, *155* (2), 206–222.
(42) Hook, F.; Kasemo, B.; Nylander, T.; Fant, C.; Sott, K.; Elwing, H. *Anal. Chem.* **2001**, *73* (24), 5796–5804.
(43) Gunning, A. P.; Chambers, S.; Pin, C.; Man, A. L.; Morris, V. J.; Nicoletti, C. *FASEB J.* **2008**, *22* (7), 2331–2339.
(44) Meyer, G.; Amer, N. M. *Appl. Phys. Lett.* **1988**, *53* (12), 1045–1047.
(45) Butt, H. J.; Jaschke, M. *Nanotechnology* **1995**, *6* (1), 1–7.
(46) Hutter, J. L.; Bechhoefer, J. *Rev. Sci. Instrum.* **1993**, *64* (7), 1868–1873.
(47) Voinova, M. V.; Rodhal, M.; Jonson, M.; Kasemo, B. *Phys. Scr.* **1999**, *59* (5), 391–396.
(48) Ralet, M. C.; Dronnet, V.; Buchholt, H. C.; Thibault, J. F. *Carbohydr. Res.* **2001**, *336* (2), 117–125.
(49) Guo, L.; Colby, R. H.; Lusignan, C. P.; Howe, A. M. *Macromolecules* **2003**, *36* (26), 10009–10020.
(50) Weinbreck, F.; de Vries, R.; Schrooyen, P.; de Kruif, C. G. *Biomacromolecules* **2003**, *4*, 293–303.
(51) Notley, S. M.; Eriksson, M.; Wagberg, L. *J. Colloid Interface Sci.* **2005**, *292* (1), 29–37.
(52) Buscher, K.; Graf, K.; Ahrens, H.; Helm, C. A. *Langmuir* **2002**, *18* (9), 3585–3591.
(53) Xu, L.; Yokoyama, E.; Watando, H.; Okuda-Fukui, R.; Kawauchi, S.; Satoh, M. *Langmuir* **2004**, *20* (17), 7064–7069.
(54) Boulmedais, F.; Ball, V.; Schwinte, P.; Frisch, B.; Schaaf, P.; Voegel, J. C. *Langmuir* **2003**, *19* (2), 440–445.
(55) Vodouhe, C.; Le Guen, E.; Garza, J. M.; Francius, G.; Dejugnat, C.; Ogier, J.; Schaaf, P.; Voegel, J. C.; Lavalle, P. *Biomaterials* **2006**, *27* (22), 4149–4156.
(56) Ravi, V.; Kumar, T. M. P.; Siddaramaiah *Indian J. Pharm. Sci.* **2008**, *70* (1), 111–113.
(57) Sukhishvili, S. A.; Granick, S. *J. Am. Chem. Soc.* **2000**, *122* (39), 9550–9551.